optica

Effects of resonant-laser excitation on the emission properties in a single quantum dot: supplementary material

O. GAZZANO[1], T. HUBER[1], V. LOO[1], S. POLYAKOV[2], E. B. FLAGG[3], AND G. S. SOLOMON[1,2,*]

[1]Joint Quantum Institute, National Institute of Standards and Technology, & University of Maryland, College Park, Maryland 20742, USA
[2]National Institute of Standards and Technology, Gaithersburg, Maryland 20899, USA
[3]Department of Physics and Astronomy, West Virginia University, Morgantown, West Virginia 26506-6315, USA
[*]Corresponding author: gsolomon@umd.edu

Published 27 March 2018

This document provides supplementary information to "Effects of resonant-laser excitation on the emission properties in a single quantum dot," https://doi.org/10.1364/OPTICA.5.000354. Monte Carlo simulations are used to match the intensity changes in resonance fluorescence with resonant laser and additional, weak non-resonant light. Simulations of two-dimensional fluorescence maps highlight differences in homogeneous and inhomogeneous broadening in elastic and inelastic scattering regimes. Finally, experimental results describe how the peak intensity and full linewidth change as function of resonant and non-resonant power.

1. MONTE CARLO SIMULATIONS

Table S1. Parameters used in the Monte Carlo simulations

Ω_r	0.23 GHz	0.30 GHz	0.47 GHz	0.65 GHz
R_{loss}	2.5 MHz	3.2 MHz	6.3 MHz	10.0 MHz
Γ	1.54 GHz			
R_{relax}	12 GHz			

We simulate the dynamic of the charge carriers inside of the quantum dot (QD) using a Monte Carlo simulation. The model contains 4 levels, two in the conduction band (CB) and two in the valence band (VB), as shown in Fig. S1. The QD VB (QD CB) ground level can contain up to two electrons (two holes) with opposite spins. The excited levels are considered as reservoirs and the number of electrons or holes is not limited.

We consider several transitions between the levels that account for pumping, relaxation capture, loss and spin flip mechanisms as show in the Fig. S1. The model is probabilistic and the events occurs with a probability proportional to their rate R. We account for the following mechanisms:

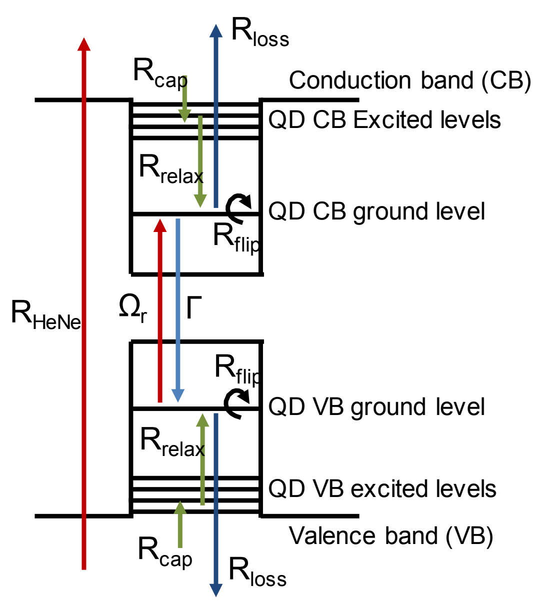

Fig. S1. Monte Carlo model. We consider a 4 level system and several mechanisms as indicated in the text of the supplementary material.

- Resonant pumping of the transition between the QD ground levels, Ω_r. This event simulates Rayleigh scattering and

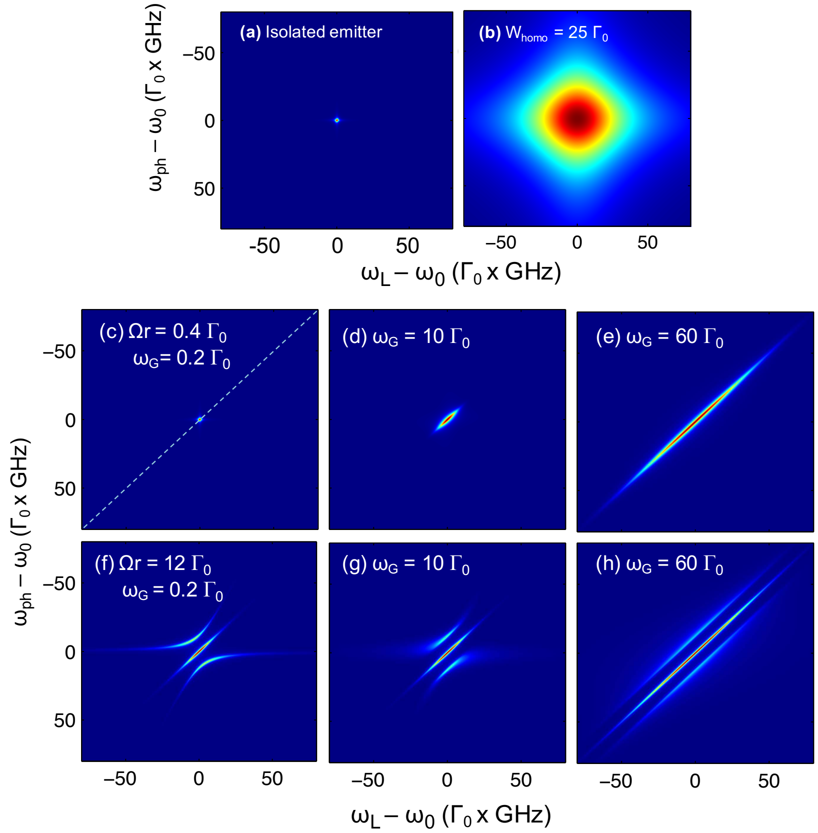

Fig. S2. Theoretical fluorescence maps in the inelastic scattering regime. (a,c,f) Case of an ideal emitter in the low pump power regime (a,c) and strong power regime (f). (b) With homogeneous broadening the map has a diamond shape. (d,e,g,h) With inhomogeneous broadening, the maps are convoluted by a Gaussian in the diagonal axis to account for the spectral wandering of the emitter transition energy. For all the figures, the detector and the laser are spectrally much narrower than the QD transition linewidth, Γ_0.

scatters a photon off the transition of interest.

- Above band pumping and QD capture rate, $R_{\text{HeNe}} \cdot R_{\text{cap}}$. This event generates an electron or a hole in the CB excited levels or the VB excited levels with random spin.
- Radiative recombination of an electron-hole pair of the QD ground levels, Γ. This leads to the emission of a photon at a frequency that depends on the occupation of the quantum dot ground and exited levels. This event occurs only between electrons and holes of opposite spins.
- Relaxation of a charge from an excited level to the corresponding ground level, R_{relax}.
- Spin-flip of a charge. Has the additional condition in the ground state, that there is no other charge present (Pauli exclusion), R_{flip}.
- Charge-carrier loss in the CB or in the VB ground levels, R_{loss}. When this event occurs, an electron or a hole is removed from the CB or the VB ground level.

The values of the different rates that we use in the model are written in Tab. S1.

To test the model we simulated the photoluminescence of a ground state of a QD with and without resonant excitation. Both produce the expected results for a very broad range of parameters, i.e. the resonant excitation creates excitons, but no charged excitons, if the QD is empty. For example, it models the power dependence of the above-band laser in the high-power regime in Fig. 3(a) and beyond. It also can reproduce the behavior of the data measured in Ref. [1], but an asymmetric flux of h^+ and e^- is needed, as also claimed by the authors in Ref. [1].

2. FLUORESCENCE MAP IN THE INELASTIC SCATTERING REGIME

We use the detuning-dependent resonant fluorescence equations of a coherently driven two-level system [2, 3] to calculate fluorescence maps in the inelastic scattering regime. Maps without broadening are plotted in Fig. S2(a),(c),(f). In the low pump power regime ($\Omega_r < \Gamma$), the maps show a small dot centered on the QD transition frequency, ω_0 (Fig. S2(a),(c)). In the strong power regime ($\Omega_r > \Gamma$), Mollow Triplet branches appear, as visible in Fig. S2(f).

When some broadening effects are introduced in the inelastic scattering regime, the maps are modified. For homogeneous broadening, the map has a diamond shape as shown in Fig. S2(b), aligned along the horizontal (constant value of ω_{ph}) and vertical axis (constant value of ω_{L}) of the fluorescence map. The fluorescence map is not circular because the fluorescence proba-

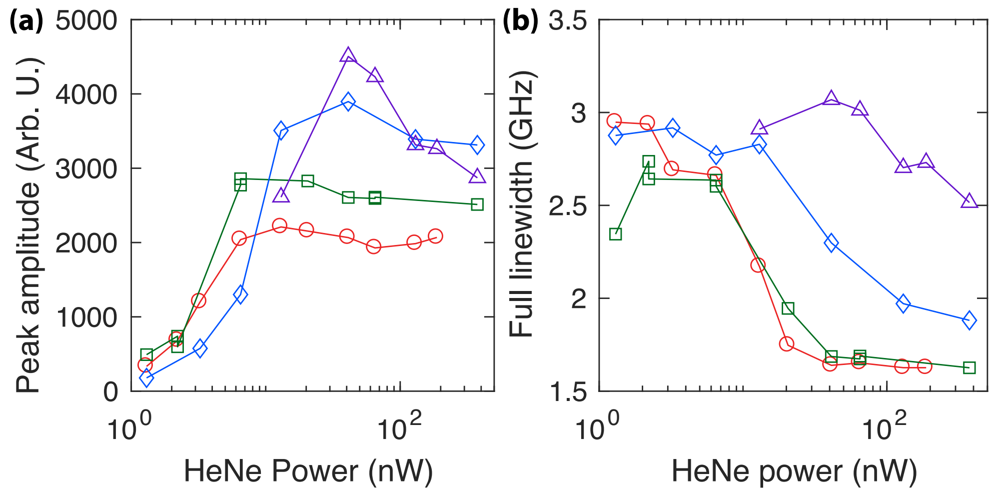

Fig. S3. Measured peak amplitude (a) and full linewidth (b) of the Voigt function fits as a function of the HeNe power and for different resonant laser powers. Red circles: $\Omega_r = 0.23$ GHz, green squares: $\Omega_r = 0.30$ GHz, blue diamonds: $\Omega_r = 0.47$ GHz, violet triangles: $\Omega_r = 0.66$ GHz.

bility is reduced for off axis points: the laser and the observed photon are detuned from the center of the transition. Thus, for pure dephasing the diamond is larger than the natural radiative linewidth but the diamond shape and orientation remains the same because the central QD transition energy is unchanged by pure dephasing.

Inhomogeneous broadening is different as it modifies the QD transition energy over a frequency range ω_G: the QD transition energy is now time dependent but can be considered constant during the emission process. The laser acts as a narrow band-pass filter since emission from the QD transition is only observed when the QD transition sweeps through the laser. The inhomogeneous broadening of the transition corresponds to a convolution of the ideal fluorescence map with a Gaussian in the diagonal axis ($\omega_{\mathrm{ph}} = \omega_{\mathrm{L}}$). Calculated maps are plotted in Figs. S2(c)-(h). for several Rabi frequencies and inhomogeneous broadenings.

If the system were in the Rayleigh (e.g. elastic) scattering regime, the map would have an oval-like shape and would be elongated along the diagonal axis ($\omega_{\mathrm{ph}} = \omega_{\mathrm{L}}$) as described in the main text and shown in Figs. 2(a),(b).

3. AMPLITUDE AND FULL LINEWIDTH

Fig. S3 represents the measured peak amplitude and the full linewidth of the Voigt function fits as a function of the HeNe power obtained for several values of the resonant laser power. These can be compared to similar data shown in Fig. 3 of the main text. For instance, in Fig. 3(a), the integrated intensity is shown, here in Fig. S3(a), the peak amplitude is shown. As with the inhomogeneous linewidth discussed in the main text (Fig. 3(b)), the full linewidth is also reduced by the effect of the above-band laser (Fig. 3(b)). There is also a delay in this reduction for increasing above-band laser power as seen in Fig. 3(b) for the inhomogeneous linewidth component.

REFERENCES

1. H. S. Nguyen, G. Sallen, C. Voisin, P. Roussignol, C. Diederichs, and G. Cassabois, "Optically Gated Resonant Emission of Single Quantum Dots," Physical Review Letters **108**, 057401 (2012).
2. B. Mollow, "Power Spectrum of Light Scattered by Two-Level Systems," Physical Review **188**, 1969–1975 (1969).
3. A. Ulhaq, S. Weiler, C. Roy, S. M. Ulrich, M. Jetter, S. Hughes, and P. Michler, "Detuning-dependent Mollow triplet of a coherently-driven single quantum dot," Optics Express **21**, 4382 (2013).